J|A|C|S
ARTICLES
Published on Web 06/09/2007

Understanding d^0-Olefin Metathesis Catalysts: Which Metal, Which Ligands?

Albert Poater,[†,‡] Xavier Solans-Monfort,[†] Eric Clot,[†] Christophe Copéret,*[,§] and Odile Eisenstein*[,†]

Contribution from the Institut Charles Gerhardt, Université Montpellier 2, CNRS, Case Courier 1501, Place E. Bataillon, Chimie Théorique, Méthodologies, Modélisations, F-34095 Montpellier Cedex 05, France, Institut de Química Computacional, Universitat de Girona, Campus de Montilivi, 17071 Girona, Spain, and C2P2, CNRS−ESCPE Lyon, Laboratoire de Chimie Organométallique de Surface, ESCPE Lyon, F-308-43 Boulevard du 11 Novembre 1918, F-69616 Villeurbanne Cedex, France

Received January 28, 2007; E-mail: odile.eisenstein@univ-montp2.fr; coperet@cpe.fr

Abstract: Density functional theory (DFT, B3PW91) calculations have been carried out on the reactivity of ethene with model systems M(≡NR)(═CHCH$_3$)(X)(Y) for M = Mo or W, R = methyl or phenyl, X = CH_2-CH_3, OCH_3, or $OSiH_3$, and Y = CH_2CH_3, OCH_3, or $OSiH_3$, which are representative of experimental olefin metathesis catalysts, and the results are compared to those previously obtained for Re(≡CCH$_3$)(═CHCH$_3$)-(X)(Y). The general pathway comprises four steps: olefin coordination, [2+2] cycloaddition, cycloreversion, and olefin de-coordination. Two key factors have been found to control the detailed shape of the energy profiles: the energy of distortion of the tetrahedral catalyst and the stability of the metallacycle intermediate, which is controlled by the M−C bond strength. The efficiency has been evaluated by calculating the turnover frequency (TOF) based on the steady-state approximation, and the most striking feature is that the unsymmetrical catalysts (X ≠ Y) are systematically more efficient for all systems (Mo, W, and Re). Overall, the Re complexes have been found to be less efficient than the Mo and W catalysts, except when Re is unsymmetrically substituted: it is then calculated to be as efficient as the best Mo and W catalysts.

Introduction

Olefin metathesis has become a key process to build carbon−carbon bonds in the development and the synthesis of pharmaceuticals, polymers, and basic chemicals. The first catalysts were based on transition-metal oxides supported on oxide surfaces. While these systems are very important in petrochemical processes,[1] they are usually incompatible with functionalized molecules, which has precluded their use in organic synthesis and material science. Since the Chauvin olefin metathesis mechanism,[2,3] based on metallocarbene and metallacyclobutane intermediates, methods for the synthesis of well-defined metallocarbene complexes based on d^0 (Mo, W or Re)[4−6] or d^4 (Ru)[7−9] transition metals have been developed. The d^0 Schrock-type catalysts, M(≡ER^1)(═CHR^2)(X)(Y) (M = Mo and W; E = N; M = Re, E = C, Scheme 1), are highly efficient olefin metathesis catalysts for a wide variety of applications from material science to asymmetric catalysis.[10,11] More recently, these catalysts have even been used for a new generation of alkane metathesis catalytic systems.[12,13] The efficiency of these olefin metathesis catalysts, typically estimated by the number of turnovers, largely depends on the nature of both the metal and the spectator ligands.[5,14] For instance, for a given X and Y pair, the catalytic efficiency normally decreases from Mo/W to Re. In addition, for a given metal, the catalytic efficiency increases with the presence of electronegative X and Y ligands; in particular, X = Y = $OC(CH_3)(CF_3)_2$ give much better catalysts than X = Y = CH_2tBu or even X = Y = O*t*Bu. These observations have led to a long-accepted idea that the more efficient catalysts are obtained by the combination of an electropositive metal with an X and Y pair of electronegative alkoxy ligands. This combination would favor the interaction

Scheme 1

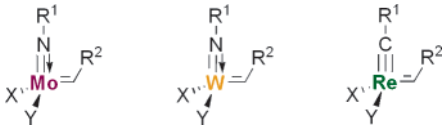

[†] Université Montpellier 2.
[‡] Universitat de Girona.
[§] ESCPE Lyon.

(1) Mol, J. C. *J. Mol. Catal. A-Chem.* **2004**, *213*, 39.
(2) Hérisson, J. L.; Chauvin, Y. *Makromol. Chem.* **1971**, *141*, 161.
(3) Chauvin, Y. *Angew. Chem., Int. Ed.* **2006**, *45*, 3740.
(4) Schrock, R. R. *Top. Organomet. Chem.* **1998**, *1*, 1.
(5) Schrock, R. R. *J. Mol. Catal. A-Chem.* **2004**, *213*, 21.
(6) Schrock, R. R. *Angew. Chem., Int. Ed.* **2006**, *45*, 3748.
(7) Grubbs, R. H.; Chang, S. *Tetrahedron* **1998**, *54*, 4413.
(8) Trnka, T. M.; Grubbs, R. H. *Acc. Chem. Res.* **2001**, *34*, 18.
(9) Grubbs, R. H. *Angew. Chem., Int. Ed.* **2006**, *45*, 3760.
(10) Hoveyda, A. H.; Schrock, R. R. *Chem. Eur. J.* **2001**, *7*, 945.
(11) Schrock, R. R.; Hoveyda, A. H. *Angew. Chem., Int. Ed.* **2003**, *42*, 4592.
(12) Goldman, A. S.; Roy, A. H.; Huang, Z.; Ahuja, R.; Schinski, W.; Brookhart, M. *Science* **2006**, *312*, 257.
(13) Blanc, F.; Copéret, C.; Thivolle-Cazat, J.; Basset, J.-M. *Angew. Chem., Int. Ed.* **2006**, *45*, 6201.
(14) Schrock, R. R. *Acc. Chem. Res.* **1990**, *23*, 158.

Scheme 2

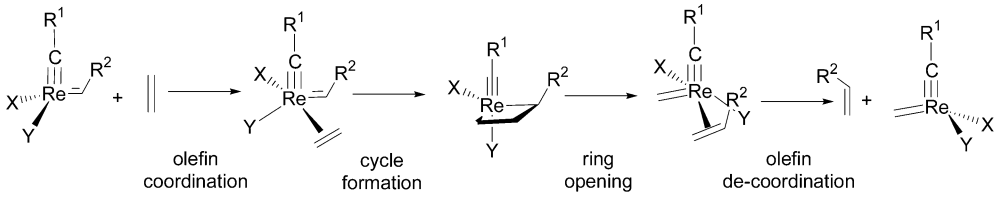

between the olefin, the Lewis base, and the electron-deficient metal, the Lewis acid.[14] However, this hypothesis does not account for the efficiency of a family of molecular and silica-grafted (R^3O)M(≡ER^1)(═CH*t*Bu)(CH_2*t*Bu) complexes (M = Mo and W; E = N; M = Re, E = C), being unsymmetrical (X = CH_2*t*Bu and Y = OR^3),[6,15−24] which are sometimes better catalysts than the symmetrical bisalkoxy complexes, M(≡ER^1)(═CH*t*Bu)$(OR)_2$.[6]

Theoretical work has focused mainly on Ru-based systems,[25−40] and in the case of d^0 complexes, theoretical studies have been focused on the catalytic activity of Mo catalysts[41−46] and especially the bisalkoxy-based complexes.[43−45] They have not addressed in detail the influence of the ancillary ligands and of the metal, with the exception of the effect of fluorine atoms in the alkoxy ligands. In all cases, the metallacycle intermediate involved in the mechanism has a trigonal bipyramid structure, although square-based pyramid isomers have also been located as minima on the potential energy surface.[47] In addition, there is some controversy about the nature of the reaction mechanism and the number of elementary steps involved (two or four). Recently, we have shown that, for d^0 Re-based catalysts, the olefin metathesis pathway consists of four steps: the coordination of the entering olefin, the metallacycle formation, and the corresponding reverse reactions (Scheme 2).[48] The energies of the intermediates and transition states are largely influenced by the nature of the X and Y ligands, the more favorable reaction pathway being obtained when X is a good *σ*-donor (alkyl) and Y a poor one (siloxy or alkoxy). This combination decreases the energy barrier of the olefin coordination/decoordination step and avoids the formation of a too stable metallacyclobutane intermediate, and thus, overall, it leads to a shallower potential energy surface.

The aim of the present work is to evaluate the scope of the four-step mechanism for d^0 complexes and to rationalize the factors that would favor the olefin metathesis reaction, paying special attention to the influence of the metal (Mo, W, and Re), the imido vs the alkylidyne, and the X and Y spectator ligands.

Computational Details

Calculations have been carried out with the hybrid B3PW91 density functional,[49,50] as implemented in the Gaussian03 package,[51] on the model systems M(≡NR^1)(═$CHCH_3$)(X)(Y) and Re(≡CCH_3)(═$CHCH_3$)(X)(Y) (R^1 = CH_3, Ph; X, Y = CH_2CH_3, OCH_3, $OSiH_3$) (Scheme 3). The Mo, W, Re, and Si atoms have been represented with the quasi relativistic effective core pseudo-potentials (RECP) of the Stuttgart group and the associated basis sets augmented with a polarization function.[52−55] The remaining atoms (C, H, N, and O) have been

Scheme 3

M-Me-1 : R^1 = CH_3, X = Y = OCH_3
M-Ph-1 : R^1 = Ph, X = Y = OCH_3
M-Me-2 : R^1 = CH_3, X = Y = CH_2CH_3
M-Ph-2 : R^1 = Ph, X = Y = CH_2CH_3
M-Me-3 : R^1 = CH_3, X = CH_2CH_3, Y = $OSiH_3$
M-Ph-3 : R^1 = Ph, X = CH_2CH_3, Y = $OSiH_3$
M-Me-4 : R^1 = CH_3, X = CH_2CH_3, Y = OCH_3
M-Ph-4 : R^1 = Ph, X = CH_2CH_3, Y = OCH_3

Re-1 : X = Y = OCH_3
Re-2 : X = Y = CH_2CH_3
Re-3 : X = CH_2CH_3, Y = $OSiH_3$
Re-4 : X = CH_2CH_3, Y = OCH_3

(15) Chabanas, M.; Baudouin, A.; Copéret, C.; Basset, J.-M. *J. Am. Chem. Soc.* **2001**, *123*, 2062.
(16) Chabanas, M.; Baudouin, A.; Copéret, C.; Basset, J.-M.; Lukens, W.; Lesage, A.; Hediger, S.; Emsley, L. *J. Am. Chem. Soc.* **2003**, *125*, 492.
(17) Chabanas, M.; Copéret, C.; Basset, J.-M. *Chem. Eur. J.* **2003**, *9*, 971.
(18) Blanc, F.; Copéret, C.; Thivolle-Cazat, J.; Basset, J.-M.; Lesage, A.; Emsley, L.; Sinha, A.; Schrock, R. R. *Angew. Chem., Int. Ed.* **2006**, *45*, 1216.
(19) Copéret, C. *New J. Chem.* **2004**, *28*, 1.
(20) Copéret, C.; Chabanas, M.; Petroff Saint-Arroman, R.; Basset, J.-M. *Angew. Chem., Int. Ed.* **2003**, *42*, 156.
(21) Rhers, B.; Salameh, A.; Baudouin, A.; Quadrelli, E. A.; Taoufik, M.; Copéret, C.; Lefebvre, F.; Basset, J.-M.; Solans-Monfort, X.; Eisenstein, O.; Lukens, W. W.; Lopez, L. P. H.; Sinha, A.; Schrock, R. R. *Organometallics* **2006**, *25*, 3554.
(22) Sinha, A.; Schrock, R. R. *Organometallics* **2004**, *23*, 1643.
(23) Pilyugina, T. S.; Schrock, R. R.; Hock, A. S.; Müller, P. *Organometallics* **2005**, *24*, 1929.
(24) Sinha, A.; Lopez, L. P. H.; Schrock, R. R.; Hock, A. S.; Müller, P. *Organometallics* **2006**, *25*, 1412.
(25) Weskamp, T.; Kohl, F. J.; Hieringer, W.; Gleich, D.; Herrman, W. A. *Angew. Chem., Int. Ed.* **1999**, *38*, 2416.
(26) Vyboishchikov, S. F.; Bühl, M.; Thiel, W. *Chem. Eur. J.* **2002**, *8*, 3962.
(27) Vyboishchikov, S. F.; Thiel, W. *Chem. Eur. J.* **2005**, *11*, 3921.
(28) Aagaard, O. M.; Meier, R. J.; Buda, F. *J. Am. Chem. Soc.* **1998**, *120*, 7174.
(29) Adlhart, C.; Hinderling, C.; Baumann, H.; Chen, P. *J. Am. Chem. Soc.* **2000**, *122*, 8204.
(30) Adlhart, C.; Chen, P. *Angew. Chem., Int. Ed.* **2002**, *41*, 4484.
(31) Adlhart, C.; Chen, P. *J. Am. Chem. Soc.* **2004**, *126*, 3496.
(32) Fomine, S.; Martinez Vargas, S.; Tlenkopatchev, M. A. *Organometallics* **2003**, *22*, 93.
(33) Fomine, S.; Vargas Ortega, J.; Tlenkopatchev, M. A. *J. Organomet. Chem.* **2006**, *691*, 3343.
(34) Cavallo, L. *J. Am. Chem. Soc.* **2002**, *124*, 8965.
(35) Correa, A.; Cavallo, L. *J. Am. Chem. Soc.* **2006**, *128*, 13352.
(36) Suresh, C. H.; Koga, N. *Organometallics* **2004**, *23*, 76.
(37) van Speybroeck, V.; Meier, R. J. *Chem. Soc. Rev.* **2003**, *32*, 151.
(38) Burdett, K. A.; Harris, L. D.; Margl, P.; Maughon, B. R.; Mokhtar-Zadeh, T.; Saucier, P. C.; Wasserman, E. P. *Organometallics* **2004**, *23*, 2027.
(39) Occhipinti, G.; Bjørsvik, H.-R.; Jensen, V. R. *J. Am. Chem. Soc.* **2006**, *128*, 6952.
(40) Jordaan, M.; van Helden, P.; van Sittert, C. G. C. E.; Vosloo, H. C. M. *J. Mol. Catal. A-Chem.* **2006**, *254*, 145.
(41) Monteyne, K.; Ziegler, T. *Organometallics* **1998**, *17*, 5901.
(42) Rappé, A. K.; Goddard, W. A., III. *J. Am. Chem. Soc.* **1982**, *104*, 448.
(43) Wu, Y.-D.; Peng, Z.-H. *J. Am. Chem. Soc.* **1997**, *119*, 8043.
(44) Wu, Y.-D.; Peng, Z.-H. *Inorg. Chim. Acta* **2003**, *345*, 241.
(45) Goumans, T. P. M.; Ehlers, A. W.; Lammertsma, K. *Organometallics* **2005**, *24*, 3200.
(46) Sodupe, M.; Lluch, J. M.; Oliva, A.; Bertran, J. *New J. Chem.* **1991**, *15*, 321.
(47) Folga, E.; Ziegler, T. *Organometallics* **1993**, *12*, 325.
(48) Solans-Monfort, X.; Clot, E.; Copéret, C.; Eisenstein, O. *J. Am. Chem. Soc.* **2005**, *127*, 14015.
(49) Becke, A. D. *J. Chem. Phys.* **1993**, *98*, 5648.
(50) Perdew, J. P.; Wang, Y. *Phys. Rev. B* **1992**, *45*, 13244.
(51) Pople, J. A.; et al. *Gaussian03*, Version D; Gaussian Inc.: Wallingford, CT, 2004.
(52) Andrae, D.; Häussermann, U.; Dolg, M.; Stoll, H.; Preuss, H. *Theor. Chim. Acta* **1990**, *77*, 123.
(53) Bergner, A.; Dolg, M.; Küchle, W.; Stoll, H.; Preuss, H. *Mol. Phys.* **1993**, *80*, 1431.
(54) Ehlers, A. W.; Böhme, M.; Dapprich, S.; Gobbi, A.; Höllwarth, A.; Jonas, V.; Köhler, K. F.; Stegmann, R.; Veldkamp, A.; Frenking, G. *Chem. Phys. Lett.* **1993**, *208*, 111.

represented with 6-31G(d,p) basis sets.[56] The B3PW91 geometry optimizations were performed without any symmetry constraint, and the nature of the extrema (local minima or transition states) was checked by analytical frequency calculations. The discussion of the results is based on the electronic energies *E* without any ZPE corrections, because inclusion of the ZPE corrections does not significantly modify the results. The free energy values *G*, computed with Gaussian03 at 298 K and $P = 1$ atm, are used to evaluate the relative rates using the model developed by Christiansen[57] and recently applied to theoretical studies on cross-coupling reactions by Kozuch and Shaik.[58] The atomic charges have been calculated using the natural population analysis scheme of Weinhold and co-workers,[59] and the topology of the electron density has been analyzed with Bader's atoms-in-molecules theory (AIM).[60,61]

Results

Models and General Remarks. We have studied the reaction paths of ethene metathesis with M(≡NR[1])(═CHCH$_3$)(X)(Y),[62,63] which are labeled by the nature of the metal M (**Mo** and **W**), the nature of X and Y (X = Y = OCH$_3$ for **1**, X = Y = CH$_2$CH$_3$ for **2**, X = CH$_2$CH$_3$, Y = OSiH$_3$ for **3**, and X = CH$_2$CH$_3$, Y = OCH$_3$ for **4**), and the nature of the R[1] substituent on the imido group (**Me** for NCH$_3$ and **Ph** for NPh). Thus, the systems whose reactivities have been studied are, for M = Mo and W: **M-Me-1**, R[1] = CH$_3$, X = Y = OCH$_3$; **M-Ph-1**, R[1] = Ph, X = Y = OCH$_3$; **M-Me-2**, R[1] = CH$_3$, X = Y = CH$_2$CH$_3$; **M-Ph-2**, R[1] = Ph, X = Y = CH$_2$CH$_3$; **M-Me-3**, R[1] = CH$_3$, X = CH$_2$CH$_3$, Y = OSiH$_3$; **M-Ph-3**, R[1] = Ph, X = CH$_2$CH$_3$, Y = OSiH$_3$; **M-Me-4**, R[1] = CH$_3$, X = CH$_2$CH$_3$, Y = OCH$_3$; **M-Ph-4**, R[1] = Ph, X = CH$_2$CH$_3$, Y = OCH$_3$) (Scheme 3). The complexes Re(≡CCH$_3$)(═CHCH$_3$)(X)(Y) (**Re-1**, X = Y = OCH$_3$; **Re-2**, X = Y = CH$_2$CH$_3$; **Re-3**, X = CH$_2$CH$_3$, Y = OSiH$_3$; **Re-4**, X = CH$_2$CH$_3$, Y = OCH$_3$), whose reactivities have been previously studied,[48] are included for comparison. For convenience, the notation **M-*i*** (M = Mo, W, or Re; *i* = 1−4) will be used when the nature of the imido or alkylidyne group does not need to be specified.

As previously discussed in earlier works, all these complexes (Mo, W, and Re) present a pseudo-tetrahedral geometry, in which the imido or alkylidyne, the metal, the alkylidene C$_{ene}$, and the substituent on the alkylidene group (Me) are coplanar.[62,64] This leads to two possible isomers (*syn* and *anti*), the *syn* being the most stable. Finally, the imido and the alkylidyne are triply bonded to the metal center, as evidenced by AIM and natural bond order analyses.

In olefin metathesis, the alkene must approach *cis* to the alkylidene ligand. Therefore, only three of the four possible approaches (*front*, *back*, and *bottom*) to the triangular faces of the tetrahedron are reactive (Scheme 4). The *front* and *back* approaches are equivalent when X and Y are the same. The *bottom* approach, which requires the rotation of the alkylidene group, is a high-energy process and has not been studied.[62,64−68] Consequently, only one attack has to be considered when X = Y, and both *front* and *back* attacks have been studied for X ≠ Y.

Scheme 4

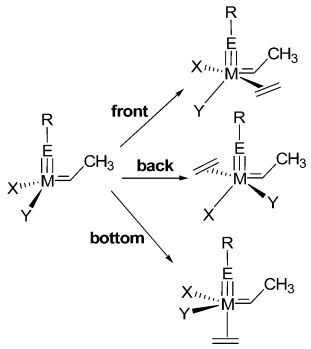

Ethene Metathesis Pathway. The four-step pathway (Scheme 5), previously obtained for Re-based catalysts,[48] also applies for all d^0 group 6 catalysts: coordination/de-coordination of the olefin and metallacycle formation/opening (Tables 1 and 2). In some specific cases (**Mo-Ph-1**, **Mo-Ph-2**, **W-Me-1**, **W-Ph-1**, and **W-Ph-2**), the olefin complex has not been found as a minimum of the potential energy surface, and thus the only localized transition states are those associated with coordination and de-coordination of the olefin (*vide infra* for further comments). The geometries of all located extrema (Figures S1−S20, Supporting Information) do not substantially change with the nature of the metal and the ligands.[69] Moreover, in contrast to our previous work on Re-based olefin metathesis catalysts, the square-based pyramidal metallacycle isomers (SP) have also been included in the study because these intermediates correspond to potential resting states (Figures S21−S23, Supporting Information).

The coordination of ethene (**I** → **II** via **TSI**) requires a change of coordination from a tetrahedron to a distorted trigonal bipyramid (TBP). At the transition state, **M-TSI**, the apical ligands are one of the ancillary ligands (X) and the entering olefin, the latter being still far from the metal center (more than 3.1 Å). The three other ligands—the imido or alkylidyne (ER[1]), the alkylidene, and Y—form the equatorial plane. In the case of **M-3**, for which X = CH$_2$CH$_3$ and Y = OSiH$_3$, the favored transition state is obtained for the *front* attack, that is, the olefin approaching *trans* to X, as already found for **Re-3**.[48] The *back* approach, which is always significantly disfavored, has therefore not been considered in the case of **M-4** (X = CH$_2$CH$_3$ and Y = OCH$_3$). At the transition state **TSI**, the metal−ligand bonds in the equatorial plane are slightly elongated, and the triply bonded ligand bends slightly, M≡E−C angle >159°. From **TSI** to the ethene complex, **II**, the TBP structure is maintained, and the major change is the shortening of the metal−olefin distance,

(55) Höllwarth, A.; Böhme, M.; Dapprich, S.; Ehlers, A. W.; Gobbi, A.; Jonas, V.; Köhler, K. F.; Stegmann, R.; Veldkamp, A.; Frenking, G. *Chem. Phys. Lett.* **1993**, *208*, 237.
(56) Hehre, W. J.; Ditchfield, R.; Pople, J. A. *J. Chem. Phys.* **1972**, *56*, 2257.
(57) Christiansen, J. A. *Adv. Catal.* **1953**, *5*, 311.
(58) Kozuch, S.; Shaik, S. *J. Am. Chem. Soc.* **2006**, *128*, 3355.
(59) Reed, A. E.; Curtiss, L. A.; Weinhold, F. *Chem. Rev.* **1988**, *88*, 899.
(60) Bader, R. F. W. *Chem. Rev.* **1991**, *91*, 893.
(61) Bader, R. F. W. *Atoms in Molecules: A Quantum Theory*; Oxford University Press: Oxford, 1995.
(62) Poater, A.; Solans-Monfort, X.; Clot, E.; Copéret, C.; Eisenstein, O. *Dalton Trans.* **2006**, 3077.
(63) In ref 62, it has been shown that the N−M bonds are best represented by a triple bond, and therefore the notation M(≡NR[1]) will be used throughout the text.
(64) Solans-Monfort, X.; Clot, E.; Copéret, C.; Eisenstein, O. *Organometallics* **2005**, *24*, 1586.
(65) Schrock, R. R.; Murdzek, J. S.; Bazan, G. C.; Robbins, J.; DiMare, M.; O'Regan, M. *J. Am. Chem. Soc.* **1990**, *112*, 3875.
(66) Schrock, R. R.; Crowe, W. E.; Bazan, G. C.; DiMare, M.; O'Regan, M. B.; Schofield, M. H. *Organometallics* **1991**, *10*, 1832.
(67) Toreki, R.; Schrock, R. R.; Davis, W. M. *J. Am. Chem. Soc.* **1992**, *114*, 3367.
(68) Oskam, J. H.; Schrock, R. R. *J. Am. Chem. Soc.* **1993**, *115*, 11831.
(69) For a more detailed presentation of geometries of the extrema, see additional text in the Supporting Information.

Scheme 5

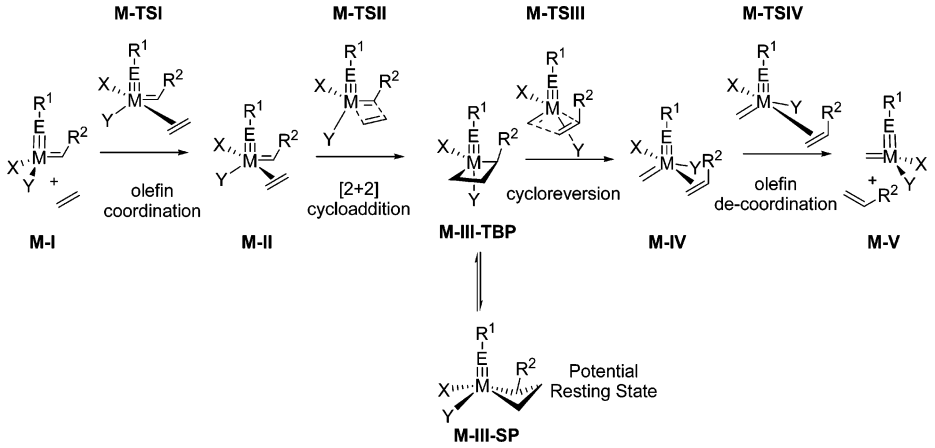

Table 1. Electronic Energy ΔE and Free Energy ΔG (kcal mol^{-1}) for the Extrema Located along the Pathways of Ethene Metathesis with Molybdenum-Based Catalysts[a]

catalyst		TSI	II	TSII	III	TSIII	IV	TSIV	V[b]
Mo-Me-1	ΔE	5.6	0.6	0.8	−13.7	3.4	3.0	5.6	−1.1
	ΔG	17.7	15.3	16.2	4.5	20.4	17.8	17.0	−1.2
Mo-Ph-1	ΔE	5.4	—[c]	—[c]	−14.4	2.7	1.9	4.8	−0.8
	ΔG	17.5	—[c]	—[c]	4.2	20.1	17.3	16.6	−0.7
Mo-Me-2	ΔE	6.0	1.9	2.9	−7.8	6.2	5.7	6.7	−0.8
	ΔG	18.9	16.9	19.9	11.5	24.2	21.5	20.5	−1.1
Mo-Ph-2	ΔE	4.9	—[c]	—[c]	−8.4	6.0	5.1	5.9	−0.5
	ΔG	16.2	—[c]	—[c]	10.7	23.9	21.1	19.8	−1.7
Mo-Me-3$_{front}$	ΔE	0.8	−0.4	0.9	−13.4	4.2	0.6	0.6	−0.8
	ΔG	12.0	14.1	17.7	4.9	21.2	12.9	13.8	−0.6
Mo-Me-3$_{back}$	ΔE	16.9	—[d]	—[d]	—[d]	—[d]	—[d]	—[d]	—[d]
	ΔG[d]	30.8	—[d]	—[d]	—[d]	—[d]	—[d]	—[d]	—[d]
Mo-Ph-3	ΔE	0.3	−1.0	0.7	−13.7	4.4	0.1	0.2	−0.6
	ΔG	12.3	14.0	18.0	4.8	21.8	13.9	13.0	−0.6
Mo-Me-4	ΔE	1.0	0.1	1.4	−13.1	4.3	0.6	0.6	−1.3
	ΔG	12.0	13.8	17.9	5.2	20.6	12.9	13.0	−1.0
Mo-Ph-4	ΔE	0.3	−0.7	0.9	−13.6	4.3	−0.2	0.0	−1.0
	ΔG	12.1	13.1	17.5	4.0	21.3	12.6	12.0	−1.3

[a] See Scheme 3 for catalyst labeling. All energies are given with respect to **I** corresponding to the separated reactants, Mo(≡NR^1)(=CHCH$_3$)(X)(Y) and C_2H_4. [b] **V** refers to the products Mo(≡NR^1)(=CH$_2$)(X)(Y) + C_3H_6. [c] Not located. [d] Not calculated.

Table 2. Electronic Energy ΔE and Free Energy ΔG (kcal mol^{-1}) for the Extrema Located along the Pathways of Ethene Metathesis with Tungsten- and Rhenium-Based Catalysts[a]

catalyst		TSI	II	TSII	III	TSIII	IV	TSIV	V[b]
W-Me-1	ΔE	5.9	—[c]	—[c]	−19.5	—[c]	—[c]	4.4	−2.2
	ΔG	17.6	—[c]	—[c]	−1.9	—[c]	—[c]	16.1	−2.8
W-Ph-1	ΔE	5.0	—[c]	—[c]	−20.6	—[c]	—[c]	3.5	−2.0
	ΔG	17.2	—[c]	—[c]	−2.1	—[c]	—[c]	15.4	−2.2
W-Me-2	ΔE	5.6	—[c]	1.9	−9.5	5.0	4.9	5.6	−1.7
	ΔG	19.0	—[c]	19.4	10.2	23.0	21.2	20.0	−2.0
W-Ph-2	ΔE	4.3	—[c]	—[c]	−12.2	4.6	—[c]	4.6	−1.4
	ΔG	16.6	—[c]	—[c]	9.2	22.2	20.0	18.6	−2.2
W-Me-3$_{front}$	ΔE	0.6	−1.6	−1.5	−17.0	1.6	−0.9	−0.7	−2.0
	ΔG	12.0	13.2	14.3	1.0	18.2	12.7	12.1	−2.2
W-Me-3$_{back}$	ΔE	15.4	—[d]	—[d]	—[d]	—[d]	—[d]	—[d]	—[d]
	ΔG[d]	28.9	—[d]	—[d]	—[d]	—[d]	—[d]	—[d]	—[d]
W-Ph-3	ΔE	0.1	−2.3	−2.0	−17.3	1.5	−1.8	−1.2	−1.7
	ΔG	11.6	12.5	14.5	0.8	18.2	12.7	10.8	−1.9
W-Me-4	ΔE	0.9	−1.0	−0.9	−16.5	1.9	−0.5	−0.4	−2.4
	ΔG	12.3	13.8	15.2	1.9	18.3	12.4	12.0	−2.1
W-Ph-4	ΔE	0.1	−1.8	−1.6	−17.1	1.5	−1.6	−1.4	−2.1
	ΔG	11.7	12.3	14.4	0.8	18.4	11.4	10.5	−2.5
Re-1[e]	ΔE	9.3	−1.2	—[c,]	−15.2	2.7	2.3	8.7	−1.7
	ΔG	21.8	14.3	—[c]	2.8	19.7	18.5	21.4	−1.3
Re-2[e]	ΔE	12.3	7.1	8.2	−1.0	9.4	7.9	11.9	−1.2
	ΔG	25.0	22.4	24.7	17.9	26.0	23.0	24.7	−1.3
Re-3$_{front}$[e]	ΔE	2.9	−0.2	1.7	−12.6	5.6	1.8	2.8	−0.9
	ΔG	13.1	13.7	17.4	4.2	21.7	15.6	15.4	−0.7
Re-3$_{back}$[e]	ΔE	23.3	—[d]	—[d]	—[d]	—[d]	—[d]	—[d]	—[d]
	ΔG[d]	37.3	—[d]	—[d]	—[d]	—[d]	—[d]	—[d]	—[d]
Re-4[e]	ΔE	4.4	1.4	3.7	−9.6	7.3	3.2	4.1	−1.2
	ΔG	16.5	16.1	20.6	8.2	24.0	18.1	17.5	−0.2

[a] See Scheme 3 for catalyst labeling. All energies are given with respect to **I** corresponding to the separated reactants, M(≡ER^1)(=CHCH$_3$)(X)(Y) and C_2H_4. [b] **V** refers to the separated products: M(≡ER^1)(=CH$_2$)(X)(Y) + C_3H_6. [c] Not located. [d] Not calculated. [e] Values from ref 48.

which varies from more than 3.1 Å in **TSI** to less than 2.75 Å in **II**, the triply bonded ligand remaining slightly bent (M≡E−C angle >153°) and the E≡M−Y angle increasing.

The [2+2] cycloaddition (**II** → **III** via **TSII**) takes place through a slight haptotropic shift of the ethene from η^2 in **II** to η^1 in **TSII**, which reduces the C···C and the Mo···C distances of the bonds to be formed (the average variations are 0.43 and 0.23 Å, respectively). Conversely, the M=C and C=C bond lengths slightly increase, while the E≡M−Y angle opens by less than 10°. The metallacyclobutane intermediate obtained from **TSII** has a TBP structure (**III-TBP**) with axial imido or alkylidyne and Y ligands (E≡M−Y > 170°, with the exception of X = Y = CH_2CH_3, for which E≡M−Y > 145°, Scheme 5). From **I** to **III**, the M≡E and M−Y bond lengths increase and the triply bonded ligand still remains essentially linear, the M≡E−C angle ranging from 177.7 to 149.3°.

Although the metallacyclobutane involved directly in the ethene metathesis has a TBP structure, square-based pyramidal (SP) metallacyclobutane isomers have been found as more stable minima on the potential energy surface (Table 3 and Figures S21−23). No transition state could be located for TBP−SP interconversion, but this isomerization is expected to be facile (low activation energy). In these complexes, the metallacycle is in the basal plane, while ≡ER, X, or Y occupies the apical site. The most stable structures have ER as an apical ligand (**SP-ER**), with the exception of **Mo-2** and **W-2**, for which the favored apical ligand is an alkyl group (**SP-X**) (Scheme 6). In all cases, the geometrical features of these SP isomers are similar and in agreement with the existing X-ray structures of several bisalkoxy metallacyclobutanes.[70−73] The most significant dif-

(70) Feldman, J.; Davis, W. M.; Schrock, R. R. *Organometallics* **1989**, *8*, 2266.
(71) Feldman, J.; Davis, W. M.; Thomas, J. K.; Schrock, R. R. *Organometallics* **1990**, *9*, 2535.
(72) Feldman, J.; Murdzek, J. S.; Davis, W. M.; Schrock, R. R. *Organometallics* **1989**, *8*, 2260.
(73) Schrock, R. R.; DePue, R. T.; Feldman, J.; Schaverien, C. J.; Dewan, J. C.; Liu, A. H. *J. Am. Chem. Soc.* **1988**, *110*, 1423.

Table 3. Energy and Free Energy (kcal mol^{-1}) of the **SP** and **TBP** Metallacycles Relative to Separated Reactants[a]

	SP-ER		SP-X		TBP	
catalyst	ΔE	ΔG	ΔE	ΔG	ΔE	ΔG
Mo-Me-1	−20.7	−3.7	−10.0	7.7	−13.7	4.5
Mo-Ph-1	−20.3	−2.7	−10.3	7.5	−14.4	4.2
Mo-Me-2	−12.4	4.2	−16.0	2.4	−7.8	11.5
Mo-Ph-2	−13.2	3.2	−15.4	3.5	−8.4	10.7
Mo-Me-3$_{front}$	−18.1	−0.9	−2.2	14.2	−13.4	4.9
Mo-Ph-3	−18.2	−0.4	−2.6	16.2	−13.7	4.8
Mo-Me-4	−18.4	−1.7	−4.4	11.6	−13.1	5.2
Mo-Ph-4	−18.4	−2.1	−6.5	12.9	−13.6	4.0
W-Me-1	−24.4	−8.2	−12.9	4.4	−19.5	−1.9
W-Ph-1	−24.2	−7.2	−12.7	5.3	−20.5	−2.1
W-Me-2	−14.4	2.1	−16.6	1.5	−9.5	10.2
W-Ph-2	−14.5	2.4	−16.4	1.8	−12.2	9.2
W-Me-3$_{front}$	−19.8	−3.6	−5.0	10.8	−17.0	1.0
W-Ph-3	−19.7	−3.7	—[b]	—[b]	−17.3	0.8
W-Me-4	−20.2	−4.2	−4.5	10.3	−16.5	1.9
W-Ph-4	−20.2	−3.4	−7.2	9.8	−17.1	0.8
Re-1	−21.2	−3.1	—[b]	—[b]	−15.2	2.8
Re-2	−10.9	6.0	−8.0	7.5	−1.0	17.9
Re-3$_{front}$	−17.0	−0.1	—[b]	—[b]	−12.6	4.2
Re-4	−17.3	−0.2	—[b]	—[b]	−9.6	8.2

[a] See Scheme 3 for catalyst labeling. See Scheme 5 for the labeling of the metallacycles. [b] Not located.

Scheme 6

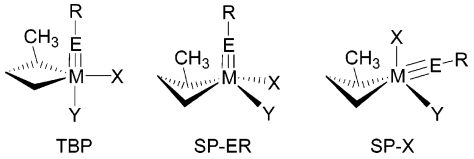

ference between SP and TBP isomers is the shape of the metallacycles: folded with the β-carbon pointing toward the apical group vs flat rings and longer M−C and shorter C−C$_\beta$ bond distances for the SP metallacycles, as previously observed experimentally and found by calculations for specific cases.[36,47,70−75]

Overall, only small geometry variations on the extrema along the ethene metathesis reaction pathway are induced by the nature of the metal and ligands. However, one significant change is an elongation of the M≡N bond upon the replacement of the methyl by a phenyl group on the imido ligand. Additionally, the replacement of the alkoxy or siloxy ligand by more σ-donor alkyl ligands yields a bending of the triply bonded ligand (imido or alkylidyne; smallest M≡E−C angle equal to 149.3° obtained for **Mo-Me-2-III**) and the formation of distorted TBP metallacyclobutane isomers with smaller E≡M−C$_Y$ angles (145° < E≡M−C$_Y$ < 155°).

The relative energies associated with ethylene metathesis and the TBP−SP isomerization of the metallacycle for all studied complexes are given in Tables 1−3 (selected potential energy surfaces are shown in Figure 1). The largest energy difference between the most stable intermediate (the SP metallacycle) and the highest point on the potential energy surface (one of the two transition states of the exit channel) is 28.8 kcal mol^{-1}, so all complexes are potentially active olefin metathesis catalysts. The energy profile depends notably on the nature of the metal and ligands. The effect of the (X,Y) ligands is similar for all metals: (a) substituting two alkoxy ligands by two alkyl groups destabilizes all intermediates and transition states (this is notably the case for the metallacyclobutane intermediates, whether in a TBP or SP geometry); (b) similarly, substituting the phenyl imido by a methyl imido ligand has also the effect of destabilizing the energies of intermediates and transition states; and (c) the unsymmetrical catalysts (**M-3** and **M-4**) have the lowest energy barriers for the coordination step (**M-3-TSI** and **M-4-TSI**), while the metallacycle intermediates, **M-3-III** and **M-4-III**, have intermediate stabilities between those of the bisalkoxy (**M-1**) and the bisalkyl (**M-2**) complexes). For 5d metals (Re vs W), substitution of the alkylidyne by the imido ligands leads to an energy profile with intermediates and transition states of lower energies. For the imido complexes, substitution of W by Mo (5d vs 4d) significantly destabilizes the metallacycle intermediates, while the transition states associated with the coordination/de-coordination steps are not affected. Overall, there is not a combination of metal and ligands that leads to a generally less energy demanding pathway. This suggests that more than one factor controls the energy profile. In particular, the accepted hypothesis, that a more electropositive metal should lead to a more efficient catalyst, is not apparent in the calculated energy profiles. It is therefore necessary to evaluate the rate of the overall process (see Overall Catalytic Cycle section) and not to focus only on individual elementary steps.

Discussion

Coordination of the Olefin and Distortion of the Catalyst. The quasi tetrahedral complexes with no empty coordination site distort into a trigonal pyramid to generate a vacant site for the incoming olefin to form a TBP complex having an axial olefin ligand. The energy barrier of the olefin coordination step depends on the energy needed to distort the initial pseudo-tetrahedral geometry into the TBP structure at **TSI** and on the affinity of the metal fragment for the incoming olefin. To understand the effect of the metal and ligands on the transition-state energies, an energy partitioning scheme of the energy barrier ($\Delta E^{\ddagger}$) has been carried out (Table 4, eq 1).[48] ΔE_{dis}(M)

$$\Delta E^{\ddagger} = \Delta E_{dis}(\mathrm{M}) + \Delta E_{dis}(//) - \Delta E_{int} \qquad (1)$$

and ΔE_{dis}(//) are respectively the energies required to distort the catalyst and ethylene from the geometries they have as isolated entities to the ones they have as fragments in the transition states; ΔE_{int} is the interaction energy between the two fragments in the transition states (calculated as the difference between $\Delta E^{\ddagger}$ and the sum of ΔE_{dis}).

At the transition state, the olefin and the metal are still far from each other (>3 Å): the C═C bond length is almost equal to that in free ethylene, leading to a negligible distortion energy of the olefin (ΔE_{dis}(//)) and to a small metal−olefin interaction (ΔE_{int}, Table 4). Thus, the energy barrier ($\Delta E^{\ddagger}$) associated with the formation of the olefin adduct is mostly determined by the distortion energy of the metal fragment from a tetrahedron into a trigonal pyramid, ΔE_{dis}(M), which is highly sensitive to the nature of X and Y ancillary ligands. For a given set of X and Y ligands, this energy is almost equal for Mo and W, indicating that the energy barrier for olefin coordination is not influenced by the nature of the metal, 4d vs 5d. The distortion energy is the highest for alkylidyne Re complexes. Distorting the metal fragment from a tetrahedron to a trigonal pyramid forces three

(74) Suresh, C. H.; Baik, M.-H. *Dalton Trans.* **2005**, 2982.
(75) Harvey, B. G.; Mayne, C. L.; Arif, A. M.; Ernst, R. D. *J. Am. Chem. Soc.* **2005**, *127*, 16426.

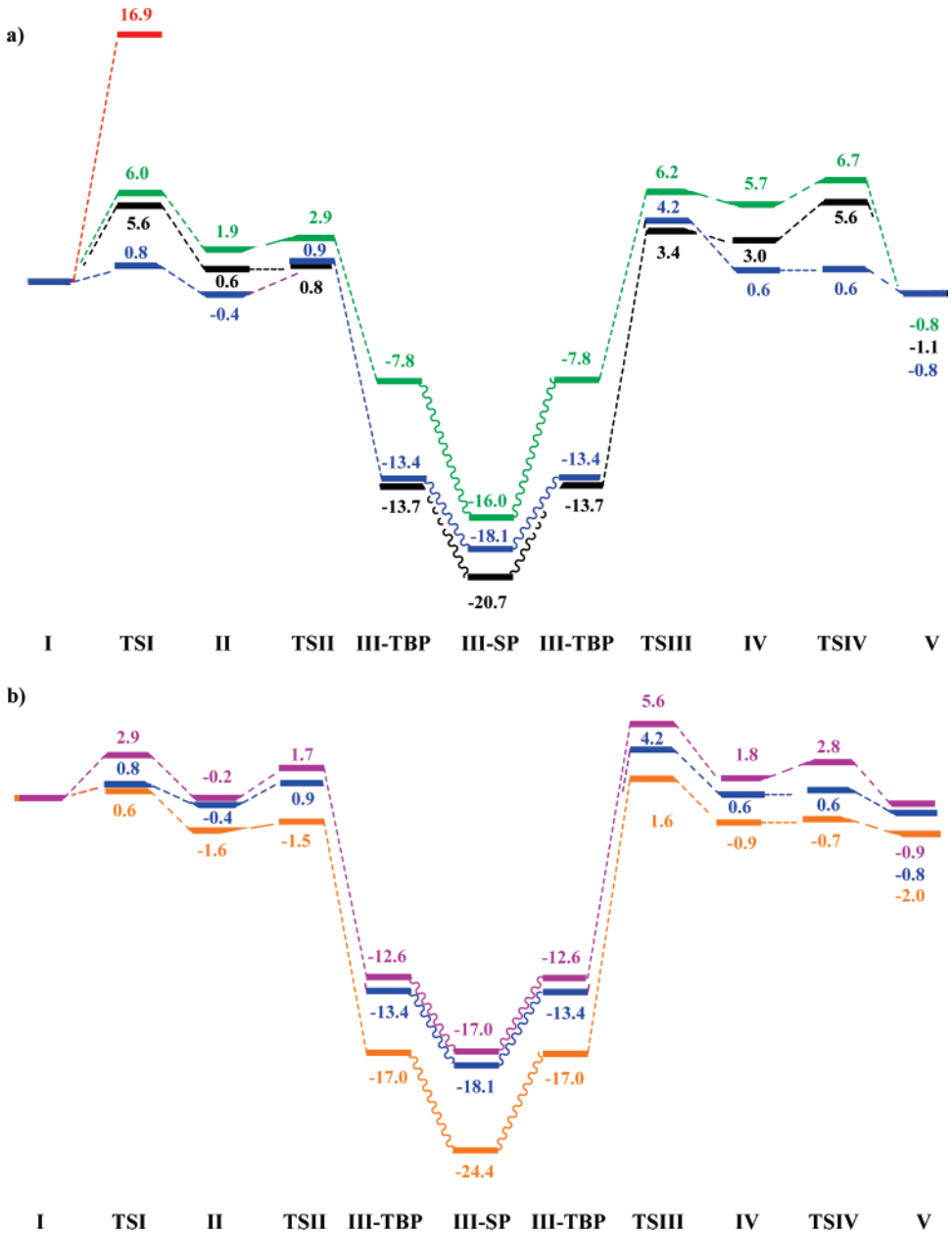

Figure 1. Potential energy surfaces (kcal mol^{-1}) for the metathesis reaction of C_2H_4 with (a) Mo(≡NCH_3)(=$CHCH_3$)(X)(Y) [X = Y = OCH_3, **Mo-Me-1** (black); X = Y = CH_2CH_3, **Mo-Me-2** (green); X = CH_2CH_3, Y = $OSiH_3$, **Mo-Me-3** front (blue) and back (red) attacks] and (b) M(≡ECH_3)(=$CHCH_3$)(CH_2-CH_3)($OSiH_3$) [M = Mo, E = N, **Mo-Me-3** (blue); M = W, E = N, **W-Me-3** (orange); M = Re, E = C, **Re-Me-3** (violet)]. For each system, the separated reactants **I** + C_2H_4 are taken as the energy origin.

ligands, including the imido or the alkylidyne, to become coplanar. This is less energy demanding when ligands have a small *trans* influence,[48] which explains the lower distortion energy of the imido complexes.[62] The difference in distortion energies and thus in energy barriers for olefin coordination to the Mo, W, and Re complexes is mostly due to the nature of the M≡ER[1] ligand (C vs N). Moreover, the effect of X and Y is similar for all metals: the energy distortion is lowered when Y, which goes into the equatorial plane of the TBP, is a poor σ-donor ligand and when X, which goes to the axial site *trans* to the entering olefin, is a good σ-donor ligand.[48] Finally, the substitution of the methyl imido by a phenyl imido further decreases the energy barrier of the olefin coordination step, because of the lower electron donor capability of the phenyl imido ligand.[62,76,77] Hence, the distortion energy for these systems increases as follows: *front*-**M-3/4** (X = CH_2CH_3, Y = $OSiH_3$ or OCH_3) < **M-1** (X = Y = OCH_3) < **M-2** (X = Y = CH_2CH_3) ≪ *back*-**M-3/4** (Y = CH_2CH_3, X = Y = $OSiH_3$ or OCH_3), the phenyl imido giving systematically lower distortion energy than the methyl imido ligand. The effect of Y is less marked on Mo and W than on Re, which is also in agreement with the imido having a weaker *trans* influence than the alkylidyne.[62]

The three π-bonds present in the initial tetrahedral complexes, the M−C π-bond from the alkylidene ligand and two M−E π-bonds (E = N for Mo and W, and E = C for Re), are not lost during the coordination step, as suggested by the overall

(76) Kaltsoyannis, N.; Mountford, P. *J. Chem. Soc., Dalton Trans.* **1999**, 781.
(77) Parsons, T. B.; Hazari, N.; Cowley, A. R.; Green, J. C.; Mountford, P. *Inorg. Chem.* **2005**, *44*, 8442.

Table 4. Analysis of the Energy Barrier for **M-TSI** (kcal mol^{-1}) in Terms of Distortion and Interaction Energies of the Reactants[a]

catalyst	ΔE(TSI)[b]	ΔE_{dis}(M)[b]	ΔE_{dis}(*II*)[b]	ΔE_{int}[b]	$\Sigma\alpha$
Mo-Me-1	5.6	6.9	0.0	−1.3	323.5
Mo-Ph-1	5.4	6.7	0.0	−1.3	322.9
Mo-Me-2	6.0	7.3	0.0	−1.3	322.0
Mo-Ph-2	4.9	6.5	0.0	−1.6	322.4
Mo-Me-3$_{front}$	0.8	1.7	0.0	−0.9	343.3
Mo-Mo-	16.9	18.3	0.2	−1.6	303.6
W-Ph-3	0.3	1.6	0.0	−1.3	342.8
W-Me-4	1.0	2.2	0.0	−1.2	344.5
W-Ph-4	0.3	1.9	0.0	−1.6	344.7
W-Me-1	5.9	6.8	0.0	−1.1	324.7
W-Ph-1	5.0	6.5	0.0	−1.5	324.2
W-Me-2	5.6	7.1	0.1	−1.6	324.1
W-Ph-2	4.3	6.1	0.0	−1.8	324.5
W-Me-3$_{front}$	0.6	1.7	0.0	−1.1	343.5
W-Me-3$_{back}$	15.4	16.9	0.2	−1.7	306.5
W-Ph-3	0.1	1.5	0.0	−1.4	342.8
W-Me-4	0.9	2.3	0.0	−1.4	343.9
W-Ph-4	0.1	1.8	0.0	−1.7	344.4
Re-Me-1	9.3[c]	9.9[c]	0.1[c]	−0.7[c]	320.3[c]
Re-Me-2	12.3[c]	13.1[c]	0.1[c]	−0.8[c]	317.5[c]
Re-Me-3$_{front}$	2.9[c]	3.5[c]	0.0[c]	−0.6[c]	337.5[c]
Re-Me-3$_{back}$	23.3[c]	23.8[c]	0.2[c]	−0.7[c]	300.7[c]
Re-Me-4	4.4[c]	5.3[c]	0.0[c]	−0.9[c]	337.1

[a] See Scheme 3 for catalyst labeling. [b] See text for definition. [c] Values taken from ref 48.

Scheme 7

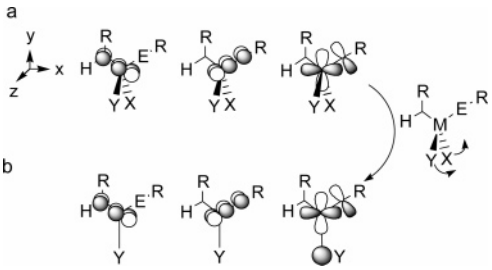

large M−N−R^1 angle and the computed AIM ellipticity (Tables S1−S20, Supporting Information). In the initial tetrahedral complex, these three π-bonds are based on three metal orbitals that are either nonbonding or slightly antibonding with the other ligands (Scheme 7a). In **TSI**, whose metal fragment has a trigonal pyramid geometry, the metal−alkylidene and the M≡E π-bond, perpendicular to the basal plane, use nonbonding d_{xz} and d_{yz} orbitals, and the other M≡E π-bond, in the basal plane, uses a $d_{x^2-y^2}$ orbital, which is antibonding with the Y ligand (Scheme 7b). The $d_{x^2-y^2}$ orbital is therefore destabilized by σ-donor Y ligands, which, in turn, increases the energy gap between the empty $d_{x^2-y^2}$ orbital and the occupied p orbital of the triply bonded E ligand. Thus, the M≡E π interaction becomes weaker and the electron density of the M≡E bond is polarized toward E on going from **M-I** to **M-II**, especially for σ-donor Y ligands. The decrease in the $d_\pi-p_\pi$ interaction is more unfavorable for the alkylidyne ligand, because the less electronegative alkylidyne ligand cannot localize the electron density on E as well as the imido ligand. To compensate the bond polarization toward E, the M≡E−R^1 angle bends slightly without ever forming a localized lone pair at E. This is supported by AIM (*vide supra* and Tables S1−S20) and by the shape of the molecular orbitals shown in Figures S24.

Olefin Adduct and Ring Formation (C−C Coupling). The olefin adduct **M-II** has not been found as a local minimum for some catalysts (**W-Me-1** and **M-Ph-1**, **M-Ph-2**). For all other complexes, the relative energies of **M-II** with respect to separated reactants range from −2.3 kcal mol^{-1} for **W-Ar-3** to +7.1 kcal mol^{-1} for **Re-2**, the bisalkyl alkylidyne−alkylidene rhenium complex. The relative stability of **M-II** for a given metal, as a function of X and Y ligands, follows the trend found for **M-TSI** and varies in general as follows: unsymmetrical systems (alkyl/siloxy, **M-3-II**, or alkyl/alkoxy, **M-4-II**), bisalkoxy complexes (**M-1-II**), bisalkyl complexes (**M-2-II**), with the exception of **Re-1-II**, which is more stable than **Re-3-II**. Overall, these similar effects suggest that the stability of **M-II** is still controlled by the distortion energy of the metal fragment as in **TSI**, although the affinity of the metal for the incoming olefin starts to have a role, as evidenced by the effect of the metal (5d metals lead to stronger M−L interactions than 4d metals[78,79]). For given X/Y ligands, the relative stability of **M-II** decreases in the order W > Mo > Re, which differs from that found for **M-TSI** (Mo ≈ W > Re), and this shows that metal olefin complexes **M-II** are stabilized for 5d metals more than **M-TSI**.

The energy barriers for the [2+2] cycloaddition via **M-TSII** are always low or even very low (≤2.3 kcal mol^{-1}). They are lower for W than for Mo and Re, and they are also lower for the bisalkoxy complexes, **M-1**. As a result, the barrier disappears for **W-1**. The energy barriers parallel the stabilities of the metallacycles, as expected for a strongly exothermic transformation (Hammond postulate).

Metallacyclobutane and Ring Opening (C−C Cleavage). The metallacyclobutanes, with either TBP (**M-III**) or SP geometries, are more stable than the separated reactants. Both the TBP and SP isomer stabilities follow the same trends, and they depend on the nature of the metal and the ligands. The metallacycles are significantly more stable for W than for Mo and Re for a given set of X and Y ligands. For any metal, the least stable metallacyclobutanes correspond to the bisalkyl **M-2** systems. The most stable metallacyclobutanes are those of the bisalkoxy complexes, **M-1**, and those of **M-3** and **M-4** catalysts have intermediate stabilities. This shows the destabilizing role of stronger σ-donor ligands such as alkyls.

In order to understand in detail the relative stability of the metallacycles, an energy partitioning scheme was devised in terms of a thermodynamic cycle shown in Scheme 8 and associated values given in Table 5.[80] The formation of the

Scheme 8

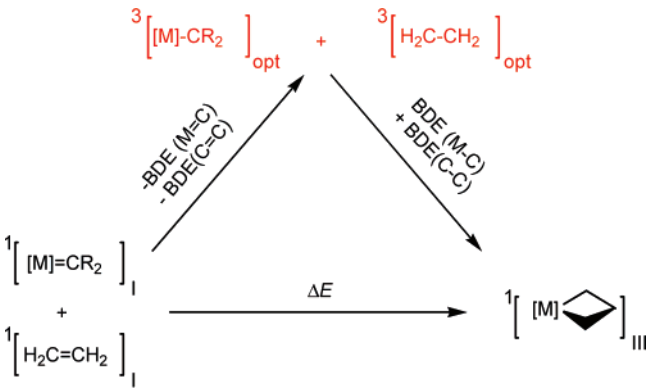

(78) Simões, J. A. M.; Beauchamp, J. L. *Chem. Rev.* **1990**, *90*, 629.
(79) Ohanessian, G.; Goddard, W. A., III. *Acc. Chem. Res.* **1990**, *23*, 386.
(80) Tomàs, J.; Lledós, A.; Jean, Y. *Organometallics* **1998**, *17*, 4932.

Table 5. Energies (kcal mol^{-1}) Associated with the Thermodynamic Cycle As Described in Scheme 8[a]

			TBP		SP	
catalyst	BDE(C═C)	BDE(M═C)	ΔE	BDE(M–C) + BDE(C–C)	ΔE	BDE(M–C) + BDE(C–C)
Mo-Me-1	−61.8	−32.0	−13.7	−107.5	−20.7	−114.5
Mo-Ph-1	−61.8	−30.4	−14.4	−106.6	−20.3	−112.5
Mo-Me-2	−61.8	na[b]	−7.8	na[b]	−16.0	na[b]
Mo-Ph-2	−61.8	−31.3	−8.4	−101.5	−15.4	−108.5
Mo-Me-3$_{front}$	−61.8	−32.1	−13.4	−107.3	−18.1	−112.0
Mo-Me-3$_{back}$	−61.8	—[c]	—[c]	—[c]	—[c]	—[c]
Mo-Ph-3	−61.8	−30.8	−13.7	−106.3	−18.2	110.8
Mo-Me-4	−61.8	−32.1	−13.1	−107.1	−18.5	112.4
Mo-Ph-4	−61.8	−30.9	−13.6	−106.2	−18.5	111.2
W-Me-1	−61.8	−37.5	−19.5	−118.8	−24.4	−123.7
W-Ph-1	−61.8	−36.2	−20.6	−118.6	−24.2	−122.2
W-Me-2	−61.8	na[b]	−9.5	na[b]	−16.6	na[b]
W-Ph-2	−61.8	−36.3	−10.2	−108.2	−16.4	−114.5
W-Me-3$_{front}$	−61.8	−37.1	−17.0	−115.9	−19.8	−118.7
W-Me-3$_{back}$	−61.8	—[c]	—[c]	—[c]	—[c]	—[c]
W-Ph-3	−61.8	−36.0	−17.3	−115.2	−19.8	−117.6
W-Me-4	−61.8	−37.4	−16.5	−115.7	−20.2	−119.4
W-Ph-4	−61.8	−35.9	−17.1	−114.8	−20.2	117.9
Re-Me-1	−61.8	−33.5	−15.2[c]	−110.6	−21.2	−116.5
Re-Me-2	−61.8	−39.0	−1.0[c]	−101.9	−10.9	−111.7
Re-Me-3$_{front}$	−61.8	−35.8	−12.6[c]	−110.3	−17.0	−114.6
Re-Me-3$_{back}$	−61.8	—[c]	—[c]	—[c]	—[c]	—[c]
Re-Me-4	−61.8	−35.3	−9.6	−106.8	−17.3	−114.4

[a] See Scheme 3 for catalyst labeling. [b] The most stable triplet does not correspond to the M═C cleavage. [c] Not considered.

metallacycle from separated reactants is associated with the disappearance of the M═C and C═C π-bonds and the formation of M−C and C−C σ-bonds. Thus, the stabilities of the metallacyclobutanes have been studied by evaluating the bond dissociation energies (BDEs) of the M═C/C═C π-bonds and the M−C/C−C σ-bonds. For **M-I** and ethene, the BDEs of the M═C and C═C π-bonds have been calculated from the energy differences between their respective optimized triplet and singlet structures (eqs 2 and 3). The BDEs of the M−C and C−C σ-bonds cannot be calculated separately. On the other hand, the sum of the energies of the two σ-bonds, $\sum$[BDE(C−C) + BDE(M−C)], evaluated by eq 4, can be directly correlated to BDE(M−C) because the BDE of the C−C bond is most likely constant.

$$\mathrm{BDE(C{=}C)} = E^{3}_{C_2H_4} - E_{C_2H_4} \quad (2)$$

$$\mathrm{BDE(M{=}C)} = E^{3}_{M-I} - E_{M-I} \quad (3)$$

$$\sum[\mathrm{BDE(C{-}C)} + \mathrm{BDE(M{-}C)}] = (E^{3}_{M-I} + E^{3}_{C_2H_4}) - E_{M-III} \quad (4)$$

where E_{M-III} is the energy of metallacyclobutane **M-III**, E^3_{M-I} is the energy of **M-I** in its optimized triplet state,[81] and $E^3_{C_2H_4}$ is the energy of ethene in its optimized triplet state.

For Mo, the BDE(M═C) is almost independent of the X and Y ligands; therefore, the stabilization of the metallacyclobutane is entirely associated with the energy of the newly formed σ-bonds {$\sum$[BDE(C−C) + BDE(M−C)]}, which is similar for all sets of ligands (−106.2 to −107.3 kcal mol^{-1}), except for the bisalkyl complexes, for which it is much lower (−101.5 kcal mol^{-1}). The specific case of the bisalkyl complex is due to the strong σ-donor effect of the alkyl ligand, which competes with other ligands for the same metal d orbitals and hence weakens the Mo−C bonds of the metallacycle.

The same trend is obtained for W. Comparing Mo to W shows that a stronger M−C π-bond is lost in the case of **W-I** (Table 5), but it is replaced by even stronger σ-bonds in **W-III**, as expected on going from a 4d to a 5d metal.[78,79] Losing a M═C π-bond and gaining a M−C σ-bond is more stabilizing for W than for Mo because of the larger M-ligand overlap in a σ-bond, so that, overall, the metallacyclobutane is more stable for W than for Mo. The Re alkylidyne complexes show the same overall trend, but the BDE(Re═C) is more sensitive to the ligands. The $\sum$[BDE(C−C) + BDE(M−C)] values are between those of Mo and W because it combines the effect of a 5d metal, which stabilizes the metallacycle, and the presence of the strongly electron-donating alkylidyne ligand, which weakens the newly formed metal−carbon bonds in the metallacycle.

From **M-III**, cycloreversion goes through **M-TSIII**, which is always higher in energy than **M-TSII**, but which, as expected, varies similarly to **M-TSII** upon change of metals and ligands. When **TSIII** could not be located, like in the case of the bisalkoxy complexes (**W-1**), the decomposition of the metallacyclobutane occurs directly through **TSIV**. Because the TBP and SP metallacyclobutanes are probably interconverting rapidly, the activation barrier for cycloreversion should probably be considered as the difference in energy between the transition state **M-TSIII** and the most stable metallacyclobutane (**SP**). For a given metal, the smallest energy barrier is always that for the bisalkyl species, and the highest for the bisalkoxy complexes. The energy barrier for cycloreversion is mostly controlled by the stability of the metallacyclobutane, thus the M−C bond strength. An additional noticeable result is that **M-TSIII** (TS for cycloreversion) is the highest point on the exit channel for all unsymmetrical complexes **M-3**/**M-4** as well as for **M-Ph-2** (M = Mo and W).

Olefin Adduct and Olefin Dissociation. The olefin complexes **M-IV** and the transition states for olefin dissociation,

(81) It has been verified that the triplet localized one electron on the metal and one electron on the carbon.

M-TSIV, have strong similarities with **M-II** and **M-TSI**, respectively. For **W-1**, the propene adduct **W-1-IV** has not been located, like in the entry channel (**W-1-II**), probably because of the high endothermicity of the cycloreversion step, and in this case the metallacyclobutane is linked directly to the products via **M-TSIV**. The energy trends for **M-IV** and **M-TSIV** are equivalent to those reported for **M-II** and **M-TSI**, with the most stable extrema found for unsymmetrical phenyl imido complexes (X = CH_2CH_3, Y = OR) and the least stable system being the bisalkylrhenium complex, **Re-2**. Because the olefin coordination (**M-TSI** and **M-II**) and olefin de-coordination (**M-IV** and **M-TSIV**) are reverse reactions associated with the same elementary step, the analysis carried out for **M-TSI** and **M-II** applies to **M-IV** and **M-TSIV**: the distortion of the metal fragment controls the energy of **M-TSIV**.

Overall Catalytic Cycle. The pathways described in this work correspond to the metathesis of an ethylidene metal complex with ethene. Changing the nature of the alkylidene group and of the olefin will change the height of the barriers and the reaction energies. Yet, the influence of the metal and spectator ligands should be similar for any alkylidene/alkene set, so a discussion of the relative efficiency of these catalysts based on these sets of calculations can be undertaken.

First, the barriers are all accessible and relatively similar for Mo, W, and Re, independent of the sets of ligands, so none of these catalysts can be readily selected or discarded. The shape of the potential energy surface is influenced by the nature of the metal and the ligands. In particular, the existence or the absence of an olefin adduct intermediate is due to the interplay between the energy needed for distorting the catalyst (coordination/de-coordination) and the stability of the metallacyclobutane intermediate, which is controlled by the M−C bond strength. For very stable metallacyclobutanes, the transition states associated with the cycloaddition/cycloreversion steps are either located at a lower energy than these for coordination/de-coordination or not even found. For example, in the case of 5d metals having two alkoxy ligands, only two steps, which correspond to the olefin coordination and de-coordination, were identified. Overall, the potential energy surface is under the influence of two key parameters: ease of distortion of the tetrahedral catalyst and stability of the metallacyclobutane. The former is minimized by the presence of two ligands of different electron-donating ability, e.g., C- and O-based ligands, and the latter, which depends on the M−C bond strength, increases with the number of O-based ligands.

In order to evaluate which metal and ligand sets make a more efficiency catalyst, the relative rates (rr) have been calculated on the basis of the steady-state approximation.[57,58,82] The calculations of rates use the Gibbs free energy profiles (ΔG), obtained through DFT calculations on the extrema located on the potential energy surfaces (E, see Tables 1−3). The relative rates using **Mo-Me-1** as a reference, presented in Table 6, have been calculated from the free energies of the reactants (the origin for the free energies); the most stable intermediate, the SP metallacyclobutane (t); the products (ΔG); the transition state having the highest free energy in the entry (x); and the difference in free energies between the highest transition state in the exit channel and the most stable metallacycle (y). No solvent effect has been included because no charged species are involved, and all catalysts are isostructural. When four elementary steps are still found in ΔG, it was verified that the same results are obtained whether using a four-step or a two-step reaction pathway involving only the lowest minima and highest maxima. This means that the presence of the olefin adduct on the potential energy surface does not influence the calculated relative rates.

Table 6. Relative Rates (rr = r/r_0)[a] for the Reaction of Ethene with **M-I** with Respect to **Mo-NMe-1** (All Energy Values Are Given in kcal mol^{-1})

catalyst	x[b]	t[c]	y[d]	ΔG[e]	rr	rr_{M-}/rr_{M-2}
Mo-NMe-1	17.7	−3.7	24.1	−1.2	1.0	1.2
Mo-NPh-1	17.5	−2.7	22.8	−0.7	7.2	4.7
Mo-NMe-2	19.9	2.4	21.8	−1.1	0.81	1.0
Mo-NPh-2	16.2	3.2	20.4	−1.7	1.5	1.0
Mo-NMe-3	17.7	−0.9	22.1	−0.6	18	2.2×10^1
Mo-NPh-3	18	−0.4	22.2	−0.6	12	7.8
Mo-NMe-4	17.9	−1.7	22.3	−1.0	19	2.3×10^1
Mo-NPh-4	17.5	−2.1	23.4	−1.3	3.2	2.1
W-NMe-1	17.6	−8.2	24.3	−2.8	0.73	1.1×10^{-1}
W-NPh-1	17.2	−7.2	22.6	−2.2	9.6	3.5×10^{-1}
W-NMe-2	19.4	1.5	21.5	−2.0	6.7	1.0
W-NPh-2	16.6	1.8	20.4	−2.2	27	1.0
W-NMe-3	14.3	−3.6	21.8	−2.2	56	8.4
W-NPh-3	14.5	−3.7	21.9	−1.9	47	1.7
W-NMe-4	15.2	−4.2	22.5	−2.1	17	2.5
W-NPh-4	14.4	−3.4	21.8	−2.5	56	2.0
Re-1	21.8	−3.1	22.8	−1.3	0.42	1.2×10^1
Re-2	25.0	6.0	20.0	−1.3	0.034	1.00
Re-3	17.4	−0.1	21.8	−0.7	22	6.4×10^2
Re-4	20.6	−0.2	24.2	−0.2	0.16	4.7

[a] The analytical expression for the relative rate with respect to the rate for **Mo-NMe-1** (r_0) as a reference is $r = r_0(1 - e^{\Delta G/RT})/(e^{(\Delta G - t + x)/RT} + e^{y/RT} + e^{(y+t)/RT} + e^{x/RT}$, with $r_0 = 1.397 \times 10^{-18}$ and $1/RT = 1.7$ [b] x corresponds to transition state with the highest free energy in the entry channel (Tables 1 and 2). [c] t corresponds to the free energy of the most stable metallacyclobutane (Table 3), the highest free energy in the entry channel. [d] y corresponds to the difference in free energy between t and the transition state with the highest free energy in the exit channel (Tables 1 and 2). [e] Reaction free energy.

The following trends have been found:

(1) The calculated relative rates (rr) are, in general, higher for unsymmetrical complexes (X = alkyl, Y = siloxy or alkoxy) for any metal. Comparing the rr's of **M-3** (alkylsiloxy) with respect to these of **M-2** (bisalkyl) shows the following trend (rr_{M-3}/rr_{M-2} are given in parentheses): **W-NPh-3** (1.7) < **Mo-NPh-3** (7.8) < **W-NMe-3** (8.4) < **Mo-NMe-3** (22) < **Re-3** (640), which parallels the donating influence of the multiply bonded ligand, increasing from phenylimido to alkylimido to alkylidyne. In the case of **M-4**, the trend relative to **M-2** is as follows (rr_{M-4}/rr_{M-2}): **W-NPh-4** (2.0) ∼ **Mo-NPh-4** (2.1) ∼ **W-NMe-4** (2.5) < **Re-4** (4.7) < **Mo-NMe-4** (23), which shows that the unsymmetrical alkyl alkoxy system has a smaller beneficial effect on the relative rates, except for **Mo-NMe-4**. Overall, the unsymmetrical alkyl siloxy catalysts **M-3** are notably efficient.

(2) Replacing two alkyl ligands in **M-2** by two alkoxy ligands in **M-1** can be either beneficial or detrimental, and the effect depends strongly on the metal, as shown by the rr_{M-1}/rr_{M-2} ratio (values given in parentheses): **Re-1** (12) > **Mo-NPh-1** (4.7) > **Mo-NMe-1** (1.2) > **W-NPh-1** (0.35) > **W-NMe-1** (0.11).

(3) For a given set of X/Y ligands, the phenylimido complexes have higher rr's than the corresponding alkylimido, except for the unsymmetrical complexes **Mo-3**, **Mo-4**, and **W-3**.

(4) Rhenium complexes have typically lower relative rates than the corresponding Mo and W imido catalysts. In this case,

(82) Campbell, C. T. *J. Catal.* **2001**, *204*, 520.

the very strong σ-donating alkylidyne ligand exacerbates the effect of the X and Y ligands, so that the unsymmetrical alkylsiloxy catalyst **Re-3** is calculated to be as efficient as the best Mo-based system **Mo-NMe-3** and better than **Mo-1**, having two alkoxy ligands.

Experimental data support these qualitative findings: (1) unsymmetrical systems can out-perform the parent bisalkoxide complexes;[18,21−24] (2) the best rhenium-based catalyst is the silica-supported, well-defined alkylidyne alkylidene complex, [(≡SiO)(*t*BuCH$_2$)Re(═CH*t*Bu)(≡C*t*Bu)],[15] whose performance in olefin metathesis is close to that of molecular and silica-supported Mo and W imido complexes; and (3) bisalkyl imido complexes are not unreactive *per se*, as shown recently,[18,21] but their bad performance as catalysts is due only to their instability in the presence of olefins (deactivation).

Conclusions

We have shown that the efficiency of the d^0 M(≡ER^1)(═CHR^2)(X)(Y) metathesis catalysts depends on two factors that act on different sections of the potential energy surface: the ability of the initial tetrahedral catalyst to distort to open a coordination site in order to accommodate the incoming olefin, and the stability of the metallacyclobutane intermediate, which is controlled by the M−C bond strength. The catalysts based on group 6 metals are generally more active due to the presence of the imido ligand instead of the alkylidyne, because it favors the distortion of the initial complexes. However, no unique set of X and Y spectator ligands and metal (Mo or W) is optimal for the two effects at the same time. A good compromise is reached by having catalysts that are unsymmetrical at the metal center, i.e., having different X and Y ligands: one good donor ligand (alkyl) and a poor σ-donor ligand (alkoxy and siloxy).

Research efforts in olefin metathesis have so far mainly focused on developing symmetrical catalysts (X = Y), but this work suggests that developing unsymmetrical catalysts has a great potential, and recent results already show that they are very promising.

In general, catalytic processes rarely involve a single elementary step, so catalysts with no symmetry may be a better compromise for the entire cycle. This should be kept in mind when developing catalysts even for chemical processes that do not involve the formation of chiral products.

Acknowledgment. A.P. acknowledges the Spanish Ministerio de Educación y Ciencia for a doctoral grant. X.S.-M. thanks the CNRS for a postdoctoral position and the French national computing centers, IDRIS (grants 051744 and 061744) and CINES (grant lsd2217), for a generous donation of computing time.

Supporting Information Available: Tables S1−S20, giving the natural population analysis and Bader's atoms-in-molecules analysis for all studied extrema; Figures S1−S20, giving the optimized geometries of all reaction paths; Figures S21−S23, showing all located metallacycles intermediates; Figure S24, showing the three highest occupied molecular orbitals of **Mo-Me-1**, **Mo-Me-1-TSI**, **W-Me-1**, **W-Me-1-TSI**, **Re-1**, and **Re-1-TSI**; detailed presentation of the geometries of extrema along the reaction pathways; complete ref 51; list of Cartesian coordinates, *E*, and *G* absolute values of all extrema. This material is available free of charge via the Internet at http://pubs.acs.org.

JA070625Y